Atomic Mass Engineering of Ultra-High Thermal Conductivity in Large Bandgap Materials: A Case Study with Boron Arsenide

Tingting Wang(王婷婷)[1], Xiaozhe Li(李晓哲)[1], Zhuo Ju(居卓)[1], Gang Zhang(张刚)[2], Dengke Ma(马登科)[1*], Wu Li(李武)[3,4*], and Lifa Zhang(张力发)[1*]

[1]*Phonon Engineering Research Center of Jiangsu Province, Ministry of Education Key Laboratory of NSLSCS, Center for Quantum Transport and Thermal Energy Science, Institute of Physics Frontiers and Interdisciplinary Sciences, School of Physics and Technology, Nanjing Normal University, Nanjing 210023, China*
[2]*Yangtze Delta Region Academy of Beijing Institute of Technology, Jiaxing 314019, China*
[3]*Eastern Institute for Advanced Study, Eastern Institute of Technology, Ningbo 315200, China*
[4]*Institute for Advanced Study, Shenzhen University, Shenzhen 518060, China*

(Received 12 April 2025; accepted manuscript online 15 May 2025)

Heat dissipation highly relies on the thermal conductivity (κ) of materials. Materials with large bandgaps and significant atomic mass ratios, such as BAs, SiC, and θ-TaN, have attracted considerable attention due to their potential for achieving ultra-high κ, with BAs serving as a particularly representative example due to its unique combination of large bandgap and high thermal conductivity. In this paper, the effects of atomic mass modification on phonon bandgap and κ are systematically investigated using a BAs model, accounting for both three- and four-phonon scattering processes. A 20% increase in κ can be obtained by substituting B, achieved through widening the phonon bandgap, which suppresses phonon scattering. Notably, the AAOO four-phonon scattering channel is more suppressed than the AAO three-phonon channel, leading to an increased phonon lifetime (τ). For As, κ can also be enhanced by 5% when replaced by lighter atoms, such as ^{69}As, primarily due to the increased phonon group velocity (v). We systematically clarify how atomic-mass-induced bandgap variations affect τ, v, and therefore κ in wide-bandgap systems. Our work provides a specific scheme for further improving the ultra-high κ of materials with large bandgaps, which possesses great guiding significance.

DOI: 10.1088/0256-307X/42/7/070802 CSTR: 32039.14.0256-307X.42.7.070802

1. Introduction. A critical bottleneck in power electronics and optoelectronics applications is the high density of heat generated.[1–3] New materials with ultra-high thermal conductivity (κ) have been discovered to address this problem, such as zinc blende boron arsenide (BAs),[4–6] graphene,[7,8] and θ-phase tantalum nitride (θ-TaN).[9] As the cubic structure crystal closest to diamond in κ, BAs, which is more cost-effective, has been employed as a heat sink in electronic cooling applications, attracting considerable interest.[10] The high κ of BAs mainly originates from its suppressed three- and four-phonon scattering (phonon mean-free-path $\sim$2 μm), which is due to the large acoustic-optical bandgap and its acoustic bunching.[11,12] Usually, the optical branch of the phonon dispersion is mainly influenced by light atoms, while the acoustic branch is influenced by heavy atoms.[13] Considering the significant mass ratio of atoms in BAs,[12,14,15] the small mass difference of atoms may be able to induce a large change in intrinsic κ.

Various methods to improve thermal conductivity have been extensively studied.[16–18] One way of modulating the lattice κ of a material is through engineered atom variation. Experimental and computational studies have shown that the κ of graphene,[19] carbon nanotubes,[20,21] GaN,[22] and GeC[23] can be greatly enhanced after atomic variation. The atomic mass variance modulates the intrinsic κ via modulation of acoustic and optical phonon frequencies.[24–26] Currently, the strategies to enhance κ using atomic masses are mainly based on the observation that atom variation can increase the phonon lifetime (τ) by increasing the bandgap,[22] and lighter masses of atoms can increase the phonon group velocity (v).[21,27,28] In the materials with large bandgaps such as BAs and θ-TaN, theory and experiment confirmed that an anomalous decrease in κ will occur under pressure.[29–31] The large bandgap amplifies τ; isotope substitution both alters the gap and modifies phonon v. Clarifying how these two factors interplay is essential for devising atomic-mass engineering strategies to further raise κ in wide-bandgap materials.

In this work, we systematically investigate the effect of atomic masses on the κ of a BAs model, obtain a scheme to improve the ultra-high κ of large bandgap materials, and figure out the underlying mechanism. First, we explain the principles and details of our calculations. Then, we calculate the κ for atomic substitution considering both three- and four-phonon scattering. The ultrahigh κ enhancement at room temperature and the law of simultaneous change of the three-phonon τ with the four-phonon τ were found. Finally, we explore the effect of different masses of atoms

*Corresponding authors. Email: dkma@njnu.edu.cn; wu.li.phys2011@gmail.com; phyzlf@njnu.edu.cn
© 2025 Chinese Physical Society and IOP Publishing Ltd. All rights, including for text and data mining, AI training, and similar technologies, are reserved.

on the κ at different temperatures. The underlying mechanism is explained by studying the phonon τ, v, and cumulative thermal conductivity (κ_c).

2. Computational Details. The κ is calculated by solving the phonon Boltzmann transport equation,[32] and the lattice κ along the transport direction can be expressed as

$$\kappa_{\alpha\beta} = \sum_{\boldsymbol{q}j} C_{\boldsymbol{q}j} v_{\boldsymbol{q}j,\alpha} v_{\boldsymbol{q}j,\beta} \tau_{\boldsymbol{q}j,\alpha}, \tag{1}$$

where $C_{\boldsymbol{q}j}$ is the specific heat, $v_{\boldsymbol{q}j,\alpha}$ denotes the component of the velocity in the α direction with wave vector $\boldsymbol{q}$ of the jth branch, and $\tau_{\boldsymbol{q}j,\alpha}$ represents the component of the corresponding phonon τ.[33] For zinc blende BAs, the κ tensor can be described as $\kappa_{xx} = \kappa_{yy} = \kappa_{zz} = \kappa$, while all off-diagonal terms vanish.[26,34]

The three-phonon collision matrix is solved iteratively with a conjugate-gradient algorithm, whereas the four-phonon rates obtained from the single-mode relaxation-time approximation are introduced as diagonal terms and merged with the iterated three-phonon solution through Matthiessen's rule.[11,34,35] The calculation is derived from the principle that the crystal potential can be written as a Taylor expansion as

$$E = E_0 + \frac{1}{2}\sum_{\substack{ij\\ \alpha\beta}} \Phi_{ij}^{\alpha\beta} r_i^\alpha r_j^\beta + \frac{1}{3!}\sum_{\substack{ijk\\ \alpha\beta\gamma}} \Phi_{ijk}^{\alpha\beta\gamma} r_i^\alpha r_j^\beta r_k^\gamma + \frac{1}{4!}\sum_{\substack{ijkl\\ \alpha\beta\gamma\theta}} \Phi_{ijkl}^{\alpha\beta\gamma\theta} r_i^\alpha r_j^\beta r_k^\gamma r_l^\theta + \ldots, \tag{2}$$

where r_i^α is the displacement of atom i along $\alpha(x, y, z)$ direction, E_0 is the potential energy, and the coefficients Φ of the nth-order terms are the corresponding nth-order interatomic force constants (IFCs).[36]

The harmonic and anharmonic IFCs are obtained by the finite difference method within the generalized gradient approximation, using the first-principle-based VASP package.[11,32,37–41] The optimized lattice constant a = 4.81 Å is obtained, which is in good agreement with the previous experimental (a = 4.78 Å)[4] and theoretical (a = 4.81 Å)[11] results. When substituting atoms, we first choose ^{7}B and ^{66}As, which have been observed. Then, we extend our calculations to obtain a more general pattern. In the following part, corresponding to the common isotopically pure case, $^{\mathrm{nat}}$B $^{\mathrm{nat}}$As is abbreviated as BAs, and it will be made clear when other atomic masses are used. The optimized parameters for our calculations are ENCUT = 520 eV, a 5 × 5 × 5 GAMMA grid for harmonic IFC calculations, and interactions considered up to the fifth nearest neighbor for third-order IFCs and up to the second nearest neighbor for fourth-order IFCs. Considering the possible dependence of fourth-order force constants on atomic displacements,[42] we used the Perdew–Burke–Ernzerhof pseudopotential and adopted the standard atomic displacement magnitude of 0.01 Å[43] for the extraction of fourth-order IFCs. See Supplementary Materials for more details of first principles calculations.

3. Results and Discussion. The atomic structure of BAs is shown in Fig. 1(a). The structure is constituted by two interpenetrating face-centered cubic lattices, wherein each lattice is occupied by a distinct type of atom. Its first Brillouin zone is a truncated octahedron centered on the origin of the reciprocal lattice vector $\boldsymbol{k}$, as shown in Fig. 1(b). The two atoms of BAs have a large mass ratio, so its phonon dispersion is also found to have a large bandgap and acoustic bunching,[11] and this acoustic bunching becomes loosely bound under pressure, resulting in an anomalous decrease in the κ.[30] This demonstrates that the conventional method of increasing thermal conductivity by applying pressure is ineffective for materials with ultra-high thermal conductivity because of the large bandgap.

We first examine the phonon dispersion of BAs with different atomic masses, as shown in Fig. 1(c). The phonon dispersion obtained from the common isotopically pure case, shown as the black line in Fig. 1(c), is consistent with previous calculations.[11] We have also included experimental data points in Fig. 1(c) (shown as square symbols). The experimental phonon frequencies exhibit good agreement with our calculated dispersion curves, confirming the reliability of our computational approach.[44] In common perception, the high κ of BAs is due to the large bandgap between the acoustic and optical branches that greatly suppresses phonon scattering. Because a wider gap suppresses three- and four-phonon scattering, we investigate two test cases, ^{7}B and ^{66}As, to illustrate how changing the mass ratio shifts the dispersion. The phonon dispersion obtained by atomic substitution of As and B are the blue and red dashed lines respectively. It can be seen that when changing the B atom, the phonon frequency ω of the acoustic modes remains almost unchanged while the optical modes increase significantly. When changing the As atom, the acoustic modes increase obviously compared to the optical modes. This is consistent with the general understanding that the heavy atoms dominate the acoustic modes and the light atoms dominate the optical modes;

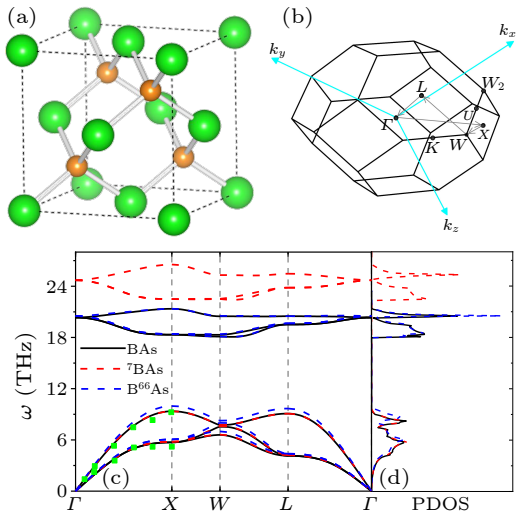

Fig. 1. (a) The crystal structure of BAs. (b) The first Brillouin zone of BAs. (c) The phonon dispersion. (d) the phonon density of states (PDOS) of BAs with different atomic masses. Here, $^{\mathrm{nat}}$B $^{\mathrm{nat}}$As is abbreviated as BAs. The square symbols represent experimental data points.[44]

the lighter atom can raise ω while the heavier atom will lower it.[23] Here, the extended bandgap, which is caused by the change in atomic mass, may further suppress the three- and four-phonon scattering and allow the κ to increase. At the same time, the increasing phonon v competes with the decreasing bandgap process. This deduction would be the subject of a more detailed discussion in the following sections.

The phonon density of states (PDOS), which describes the probability of phonon distribution in a system, is an important physical quantity for calculating the thermodynamic properties of the lattice.[45–47] Figure 1(d) gives the PDOS versus ω of BAs with different atoms. It is obtained by summing up the contribution of all phonon modes at each energy level over all $\boldsymbol{k}$-points. The formula can be written as $g(\omega) = \frac{\Omega}{(2\pi)^3}\sum_\sigma \int_{\Omega^*} \delta[\omega - \omega_\sigma(\boldsymbol{k})]\mathrm{d}^3\boldsymbol{k}$, where Ω is the per-unit volume and the integration region of the $\boldsymbol{k}$ vectors is in the first Brillouin zone. We can see that the flat optical branches have larger values of PDOS relative to the acoustic branches, and phonon localization occurs at $\omega = 21$ THz. When reducing the atomic mass of B, the phonon distribution becomes more uniform in the optical branch and is basically unchanged in the acoustic branch. If we decrease the atomic mass of As, this will be accompanied by an increase in the phonon v, which will further increase the κ. This behavior is counterintuitive, because a narrower gap usually strengthens scattering and lowers κ. To further investigate this complex mechanism, we calculate the effect of atomic masses on κ in the followings.

We then calculate the thermal conductivity at room temperature by replacing the B and As atoms, respectively, and both find an increase in thermal conductivity. As shown in Fig. 2(a), we calculate the natural κ at 300 K. The κ we calculated is 1.27 kW/mK which agrees well with the experimental results of 1.28 kW/mK.[4] Then we calculate the κ of the two atomic masses case at room temperature. It can be found that the κ of BAs increases by 20.4% when the atomic mass of B is reduced to 7, a very significant increase. When the atomic mass of As is reduced to 66, the κ of BAs increases a little as well. This result initially appears inconsistent with our expectation that a decrease in the atomic mass of As, which causes an increase in scattering rates, may lead to a decrease in κ.

The cumulative thermal conductivity (κ_c) can be used to gain insight into the distribution of κ contributors in nanostructures and is calculated as $\kappa_\mathrm{c} = \frac{1}{3}\sum_j \int_{l_{j,\min}}^{l_0} C_j v_j l_j \mathrm{d}l_j$,[48] where l_j is the phonon mean-free-path of the jth branch. Figure 2(b) illustrates the contribution of phonon frequencies to thermal conductivity for these three different atomic cases. The κ_c values here all indicate that the phonon contribution to the thermal conductivity is small in the frequency range above 10 THz, meaning that the contribution of the optical branch is negligible. The atomic substitution of B increases the acoustic branch contribution more significantly compared to As. We then compare the differences in the trends of the scattering rates of the three- and four-phonon scattering rates in the case where both κ values are increasing.

The phonon lifetime τ is the reciprocal of the phonon scattering rate, and we calculate here the trends in the three- and four-phonon τ to further elucidate the conclusion of Fig. 2. We calculate the three- and four-phonon τ for the above three different atomic cases, as shown in Fig. 3. It has been shown that three-phonon τ is smaller than four-phonon τ in the acoustic range, whereas the two lifetimes converge in the optical range. This is in good agreement with the isotopically pure case results of

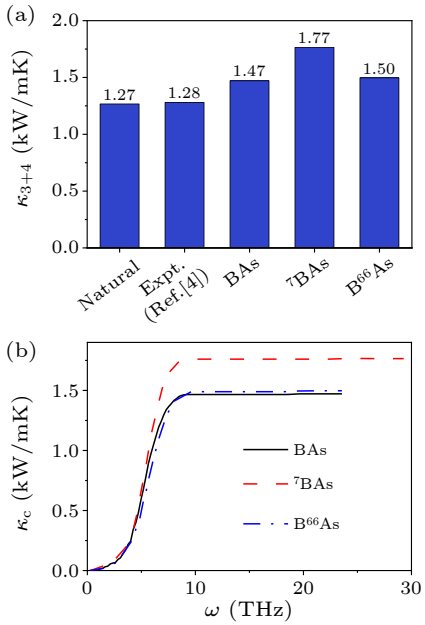

Fig. 2. (a) κ considering four-phonon scattering at different atomic masses and comparison with experimental results at 300 K. (b) Cumulative thermal conductivity κ_c versus frequency ω for BAs with different atomic masses at 300 K.

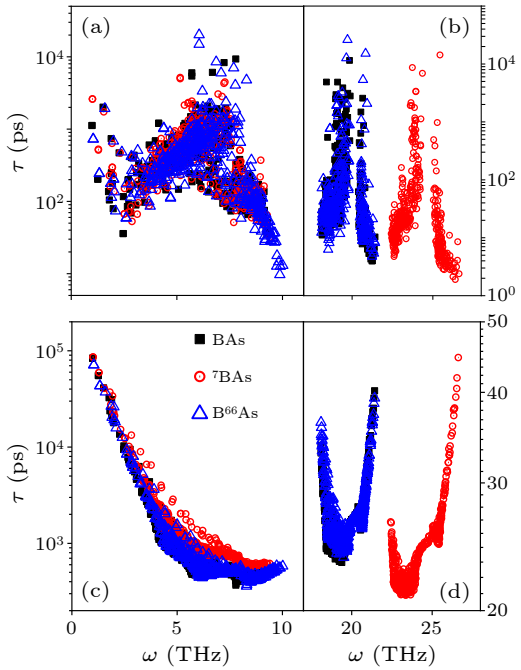

Fig. 3. (a) The acoustic part and (b) the optical part of three-phonon τ of different atomic masses. (c) The acoustic part and (d) the optical part of four-phonon τ of different atomic masses, all at 300 K.

previous calculations.[14,30] Considering that the optical branch contributes almost nothing to κ_c, we look mainly at the change in the τ of the acoustic branch. With decreasing atomic mass of B, the three-phonon τ slightly increases, while the four-phonon τ increases even more. With decreasing atomic mass of As, both the three-phonon and four-phonon τ tend to decrease.

These results reflect the different mechanisms by which the two atomic substitutions increase κ. As the atomic mass of B decreases, the acoustic branch remains almost constant while the optical branch frequency lifts. The optical branch phonon occupation number decreases, causing the scattering rate to decrease. At small bandgaps, this change mainly reduces the three-phonon scattering.[49] When the bandgap increases, the three-phonon scattering rates are reduced to the magnitude of four-phonon scattering rates. Then, the AAOO four-phonon scattering channel, which depends more on the optical branch phonon frequency, will be further suppressed. As a result, four-phonon scattering will be more strongly suppressed with a further increase in the originally large bandgap of the BAs. In contrast, decreasing the atomic mass of As decreases the bandgap, and both three-phonon scattering and four-phonon scattering increase. However, κ increases because, as the acoustic branch increases, the v of the acoustic branch is increased, which accounts for the increased κ that also occurs in the ^{66}As case. The competing mechanism of v and τ will be further shifted as the mass of the As atom continues to decrease or increase, and we provide a further discussion of this process in the following.

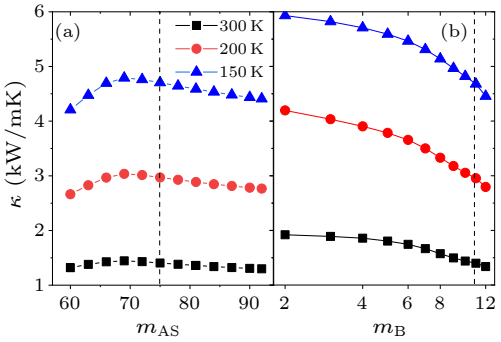

Fig. 4. The effect of atomic mass of (a) As and (b) B on κ at different temperatures T. The dashed lines mark the κ under common isotopically pure conditions.

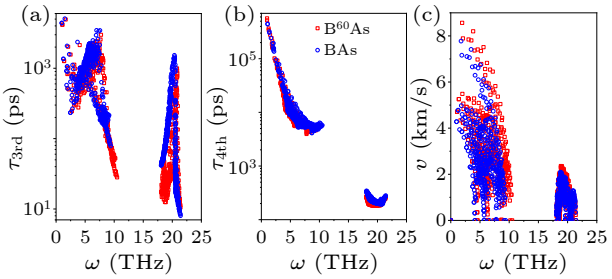

Fig. 5. (a) Three-phonon τ and (b) four-phonon τ for BAs with different atomic masses of As at 150 K. (c) Group velocities v for BAs with different atomic masses of As.

The effects of different atomic masses of B and As on κ at different temperatures are shown in Fig. 4. Figure 4(a) gives the results of κ versus the mass of As. The dashed lines mark the κ under common isotopically pure conditions. κ falls steadily as As becomes heavier, but when As is lighter, it rises, peaks near ^{69}As, and then declines. This suggests that only lighter atomic substitution can increase the κ when adjusting the atomic mass of As. In this situation, the κ of BAs can be increased by 5% when replacing As atoms at 300 K. Figure 4(b) gives the results of the κ versus the atomic mass of B. At every temperature examined, heavier B isotopes lower κ, whereas lighter isotopes raise it. The enhancement grows as temperature falls. This suggests that the ultra-high κ of BAs can be further improved by reducing the atomic mass of B, especially at low temperatures.

To investigate the underlying mechanism of the effect of bandgap changes on κ, we examine the τ and phonon v corresponding to different atomic masses of As, as shown in Fig. 5. With decreasing atomic mass of As, to make the mechanism clear enough, we choose ^{60}As at 150 K. Figure 5(a) shows the three-phonon τ; it can be seen that the τ increases slightly with decreasing atomic mass of As when $\omega \approx 22$ THz. In contrast, when $\omega \approx 10$ THz and 20 THz, the τ decreases considerably. Figure 5(b) shows the four-phonon τ; it can be found that the overall τ of ^{60}As is shorter than in the common isotopically pure case. There is much more variation in the three-phonon τ than in the four-phonon τ. Figure 5(c) shows that the phonon v increases slightly for the optical mode and increases noticeably for the acoustic mode as the atomic mass of As decreases. When the atomic mass of As decreases, the bandgap decreases; this is the reason for the changing trend in the above figures. Higher phonon v elevates κ, whereas shorter lifetimes lower it. The balance between these opposing trends shifts as atomic mass varies (see the cumulative thermal conductivity in Supplementary Materials). This results in an increase and then a decrease in κ as the atomic mass of As decreases, and a decrease in κ as the atomic mass of As increases. The above results reflect that the trend of κ is the result of the competition between phonon τ and phonon v.

4. Conclusion. In summary, our study investigates the effects of atomic mass modifications on the thermal conductivity κ of large bandgap materials using a first-principles approach. κ enhancement is observed for both atomic mass modifications in the BAs model. When modifying the mass of B and accounting for both four- and three-phonon scattering processes, a 20% enhancement of κ is achieved with lighter boron atomic mass, such as ^{7}B, compared to the isotopically pure case at room temperature, with further enhancement observed at lower temperatures. This enhancement is attributed to the widening of the phonon bandgap, which suppresses phonon scattering, particularly the AAOO four-phonon scattering channel, leading to an increase in phonon lifetime τ. At lower temperatures, four-phonon scattering is suppressed even more significantly, resulting in a greater increase in κ. For

modifications to the mass of As, decreasing the atomic mass reduces the phonon bandgap, leading to a monotonic decrease in phonon τ. However, the lifting of the acoustic phonon branch increases the phonon group velocity v. Under the combined effects of this competitive mechanism, κ initially increases slowly and then decreases. This work reveals the intrinsic mechanisms by which atomic mass modifications influence κ, deepening the understanding of ultra-high κ in materials with large atomic mass ratios and providing a new strategy for further enhancement of κ in large bandgap materials.

The data that support the findings of this study are available from the corresponding authors upon reasonable request.

Acknowledgements. This work was supported by the National Key Research and Development Program of China (Grant No. 2023YFA1407001), and the Department of Science and Technology of Jiangsu Province (Grant No. BK20220032). W. L. acknowledges support from the GuangDong Basic and Applied Basic Research Foundation (Grant No. 2023A1515010365). T. W. acknowledges support from the Postgraduate Research and Practice Innovation Program of Jiangsu Province under Grant No. KYCX25_1934.

References

[1] Cahill D G, Braun P V, Chen G, Clarke D R, Fan S, Goodson K E, Keblinski P, King W P, Mahan G D, Majumdar A *et al.* 2014 *Appl. Phys. Rev.* **1** 011305
[2] Li N, Ren J, Wang L, Zhang G, Hänggi P, and Li B 2012 *Rev. Mod. Phys.* **84** 1045
[3] Wu Y, Shi W, He C, Li J, Tang C, and Ouyang T 2024 *Appl. Phys. Lett.* **124** 202203
[4] Kang J S, Li M, Wu H, Nguyen H, and Hu Y 2018 *Science* **361** 575
[5] Li S, Zheng Q, Lv Y, Liu X, Wang X, Huang P Y, Cahill D G, and Lv B 2018 *Science* **361** 579
[6] Ouyang Y, Yu C, He J, Jiang P, Ren W, and Chen J 2022 *Phys. Rev. B* **105** 115202
[7] Balandin A A, Ghosh S, Bao W, Calizo I, Teweldebrhan D, Miao F, and Lau C N 2008 *Nano Lett.* **8** 902
[8] Ouyang Y, Zhang Z, Yu C, He J, Yan G, and Chen J 2020 *Chin. Phys. Lett.* **37** 126301
[9] Kundu A, Yang X, Ma J, Feng T, Carrete J, Ruan X, Madsen G K H, and Li W 2021 *Phys. Rev. Lett.* **126** 115901
[10] Cui Y, Qin Z, Wu H, Li M, and Hu Y 2021 *Nat. Commun.* **12** 1284
[11] Feng T, Lindsay L, and Ruan X 2017 *Phys. Rev. B* **96** 161201
[12] Broido D, Lindsay L, and Reinecke T 2013 *Phys. Rev. B* **88** 214303
[13] Zhang J, Ruf T, Cardona M, Ambacher O, Stutzmann M, Wagner J M, and Bechstedt F 1997 *Phys. Rev. B* **56** 14399
[14] Yang X, Feng T, Li J, and Ruan X 2019 *Phys. Rev. B* **100** 245203
[15] Lindsay L, Broido D A, Carrete J, Mingo N, and Reinecke T L 2015 *Phys. Rev. B* **91** 121202
[16] Sun J, Li S, Tong Z, Shao C, An M, Zhu X, Zhang C, Chen X, Wang R, Xiong Y *et al.* 2024 *Nano Lett.* **24** 10569
[17] Li S, Yu X, Bao H, and Yang N 2018 *J. Phys. Chem. C* **122** 13140
[18] Wang R, Xiong Y, Yang J, Liu Z, Li S, Chen G, Chen K, and Liu X 2024 *Mater. Today Phys.* **45** 101469
[19] Hu J, Schiffli S, Vallabhaneni A, Ruan X, and Chen Y P 2010 *Appl. Phys. Lett.* **97** 133107
[20] Shiomi J and Maruyama S 2006 *Phys. Rev. B* **74** 155401
[21] Chang C, Fennimore A, Afanasiev A, Okawa D, Ikuno T, Garcia H, Li D, Majumdar A, and Zettl A 2006 *Phys. Rev. Lett.* **97** 085901
[22] Lindsay L, Broido D, and Reinecke T 2012 *Phys. Rev. Lett.* **109** 095901
[23] Lindsay L, Broido D, and Reinecke T 2013 *Phys. Rev. B* **88** 144306
[24] Tamura S 1983 *Phys. Rev. B* **27** 858
[25] Tamura S 1984 *Phys. Rev. B* **30** 849
[26] Lindsay L 2016 *Phys. Rev. B* **94** 174304
[27] Sun H, Chen K, Gamage G A, Ziyaee H, Wang F, Wang Y, Hadjiev V G, Tian F, Chen G, and Ren Z 2019 *Mater. Today Phys.* **11** 100169
[28] Chen K, Song B, Ravichandran N K, Zheng Q, Chen X, Lee H, Sun H, Li S, Gamage G A G U, Tian F, Ding Z, Song Q, Rai A, Wu H, Koirala P, Schmidt A J, Watanabe K, Lv B, Ren Z, Shi L, Cahill D G, Taniguchi T, Broido D, and Chen G 2020 *Science* **367** 555
[29] Kundu A, Chen Y, Yang X, Meng F, Carrete J, Kabir M, Madsen G K H, and Li W 2024 *Phys. Rev. Lett.* **132** 116301
[30] Ravichandran N K and Broido D 2019 *Nat. Commun.* **10** 827
[31] He J, Yu C, Lu S, Shan S, Zhang Z, and Chen J 2023 *Nanotechnology* **35** 025703
[32] Li W, Carrete J, Katcho N A, and Mingo N 2014 *Comput. Phys. Commun.* **185** 1747
[33] Broido D, Ward A, and Mingo N 2005 *Phys. Rev. B* **72** 014308
[34] Broido D A, Malorny M, Birner G, Mingo N, and Stewart D 2007 *Appl. Phys. Lett.* **91** 231922
[35] Esfarjani K, Chen G, and Stokes H T 2011 *Phys. Rev. B* **84** 085204
[36] Shiomi J, Esfarjani K, and Chen G 2011 *Phys. Rev. B* **84** 104302
[37] Kresse G and Furthmüller J 1996 *Phys. Rev. B* **54** 11169
[38] Kresse G and Furthmüller J 1996 *Comput. Mater. Sci.* **6** 15
[39] Togo A, Oba F, and Tanaka I 2008 *Phys. Rev. B* **78** 134106
[40] Han Z, Yang X, Li W, Feng T, and Ruan X 2022 *Comput. Phys. Commun.* **270** 108179
[41] Togo A, Chaput L, Tadano T, and Tanaka I 2023 *J. Phys. Condens. Matter* **35** 353001
[42] Sun J, Liu X, Xiong Y, Yao Y, Yang X, Shao C, Wang R, and Li S 2025 *Appl. Phys. Lett.* **126** 112112
[43] Zhou H, Zhou S, Hua Z, Bawane K, and Feng T 2023 *Appl. Phys. Lett.* **123** 192201
[44] Ma H, Li C, Tang S, Yan J, Alatas A, Lindsay L, Sales B C, and Tian Z 2016 *Phys. Rev. B* **94** 220303
[45] Zhang L, Keblinski P, Wang J S, and Li B 2011 *Phys. Rev. B* **83** 064303
[46] Ma D, Zhang G, and Zhang L 2020 *J. Phys. D: Appl. Phys.* **53** 434001
[47] Yang N, Zhang G, and Li B 2010 *Nano Today* **5** 85
[48] Aketo D, Shiga T, and Shiomi J 2014 *Appl. Phys. Lett.* **105** 131901
[49] Ravichandran N K and Broido D 2021 *Nat. Commun.* **12** 3473